

# A Statistical Study of the Seismic Intensities of the 1755 Lisbon Earthquake

D.R. Brillinger and B.A. Bolt

## 1 Introduction

Substantial tragic effects result from great earthquakes – damage, deaths, tsunamis. Various groups, including seismologists, seismic engineers, government officials and insurers seek to quantify the effects in order to proceed with their work. The quantification methods employed include seismic intensity scales and damageability matrices particularly. Principal intensity scales employed are: the Modified Mercalli, (MMI), the Medvedev-Sponheuer-Karnik (MSK), and the European Macroseismic Scale. The scale values are typically denoted by roman numerals to reflect the fact that they are derived via verbal descriptions rather than some numerical physical measuring device. It is claimed that the MMI and MSK scales are similar, see e.g. (Sokolov et al. 1998).

Intensity scales are ordinal, that is the levels are qualitatively ordered and the level spacing does not matter. Adjacent categories can be merged. A probability approach is adopted and there has advantages. These include: one can examine scientific hypotheses formally, one can assess goodness of fit, one can compute and show uncertainty, one can compare alternate models, and there are often robust/resistant variants of general techniques. The broadly ranging subject matter of statistics becomes available. One is not meant to employ the intensity values using the rules of ordinary arithmetic. One purpose of this research is to examine the possibility of assessing formally if the data may be employed as if numerical-valued.

Isoseismals are often sketched on a map to indicate, generally, the seismic damage experienced. These isoseismals are meant to be contours of equal intensity, to bound areas within which the predominant intensity is the same. The lines prove useful to quantify the shaking pattern and to understand the damage. Traditionally isoseismal maps had been prepared by hand-drawing curves encompassing the observed intensities. The artist seeks to draw a curve

---

D.R. Brillinger (✉)

Statistics, University of California, Berkeley, California, USA  
e-mail: brill@stat.Berkeley.EDU

Dedicated to Bruce Bolt, friend, colleague and collaborator.

encircling, say all the *VIII* value locations, and if ignoring outlying *VIIIs*. Professor Bolt once emphasized to this writer, (Brillinger 1993), a critical aspect of existing isoseismal maps, namely that they are conservative in two senses. First, the indicated intensity level at a location is the highest noted. Second, the isoseismals themselves are drawn as far out from the source as reasonable to include all locations with given intensity. However as (Reiter 1990) states, “. . . drawing isoseismals can be a subjective process that may lead to different outcomes for different analyses.” and this provides a motivation for the present work.

(Perkins and Boatwright 1995) list some of the factors on which seismic intensities depend, namely, size of the earthquake, distance of the site from the earthquake source, the focusing of the earthquake energy and the regional and local geological effects. There is a falloff in severity of effect with distance from the source and substantial variability is inevitably present.

A prime objective of this work is to develop a statistical model involving intensities taking specific note of their ordinal character of the intensity scale data. It is anticipated that the model can be employed in probabilistic risk assessments. A principal assumption is that the dependence of the intensity on location is smooth. Related work was carried out for the 1989 Loma Prieta event in (Brillinger 1993), (Brillinger 1997), and (Brillinger et al. 2001), and for the 1994 Northridge event in (Brillinger 2003). Other researchers' papers include: (De Rubeis et al. 1992), (Pettenati et al. 1999), (Wald et al. 1999). The approach of this paper differs from that of the “other researchers” in that the ordinal nature of the MMI values is taken specific notice in an attempt to improve the results.

## 2 The Data

The concern is the Lisbon 1 November 1755 tragedy. It has been written about it as follows. This event has long held a place among the greatest in the modern world. It owes this distinction to the great destruction in Portugal, the deaths of over 60,000 people, an affected area of more than a million square miles, and the catastrophic sea wave. Actually, reports on the shaking indicate that there were three substantial, separate earthquakes within 3 hours. In the first, Lisbon was shrouded in thick dust, and the screams of the injured survivors added to the tragic scene. People in the city ran to any open space, particularly along the banks of the Tagus River. A British merchant ship was among the assembled shipping at the mouth of the Tagus. The captain described the first shock:

I felt the ship have an uncommon motion, and could not help thinking she was aground, although sure of the depth of the water. As the motion increased, my amazement increased also, and as I was looking round to find out the meaning of the uncommon motion, I was immediately acquainted with the direful cause; when at the instant I looked toward the city, I beheld the tall and stately buildings tumbling down, with great cracks and noise.

**Table 1** Observed MSK intensities and counts

<i>II</i>	<i>II+</i>	<i>III</i>	<i>III+</i>	<i>IV</i>	<i>IV+</i>	<i>V</i>	<i>V+</i>	<i>VI</i>	<i>VI+</i>	<i>VII</i>	<i>VII+</i>	<i>VIII</i>	<i>VIII+</i>	<i>IX</i>	<i>IX+</i>	<i>X</i>
5	5	11	27	128	114	104	48	111	59	84	27	29	17	13	11	17

Taken from (Bolt 2006, p. 1). That reference further goes on to say that one can speculate that the event was caused by a sudden thrust slip along the plate boundary running from the Mid-Atlantic Ridge near the Azores through the Strait of Gibraltar. The earthquake’s magnitude has been estimated as 8.7, its depth at 20–40 km and its epicentre at (–10.0, 36.5) a point about 90 km southwest of Sagres, the southwestern most point of Iberia. The data employed in the present work were provided by J. M. Miranda, who acknowledged Mezcuca. There are 810 observations in Portugal and Spain.

There is discussion of seismic damage scales in (Bullen and Bolt 1985, pp. 433–437), and (Reiter 1990). A disadvantage resulting from the scales being concerned with damage is that damage can’t occur at a given location if there is nothing there to be damaged. Other references using intensity values to understand the 1755 event include: (Mendes-Victor et al. 1999), (Baptista et al. 2003), (Martinez-Solares and Lopez-Arroyo 2004).

The counts of the numbers of the various MSK intensities recorded are provided in Table 1. There are intermediate levels, indicated by +, in the data set. Because such values are not part of the MSK scale they are not included in the analyses presented.

Figure 1 provides a histogram of the data values. One notices a lack of intensity+ values in some cases. For this reason, and because the official

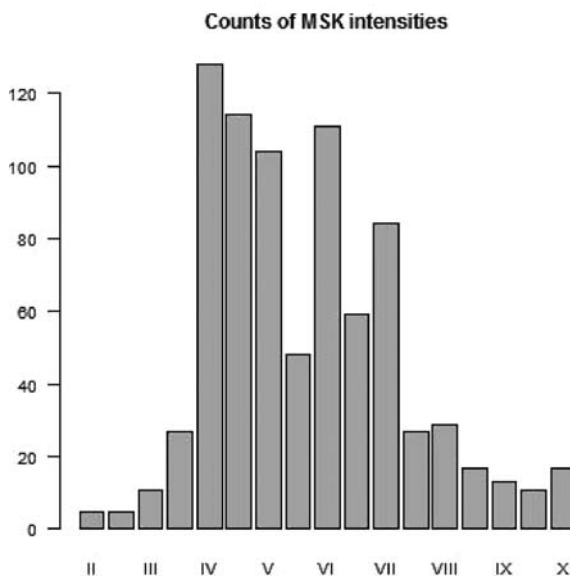


**Fig. 1** Histogram of intensity values in the data set

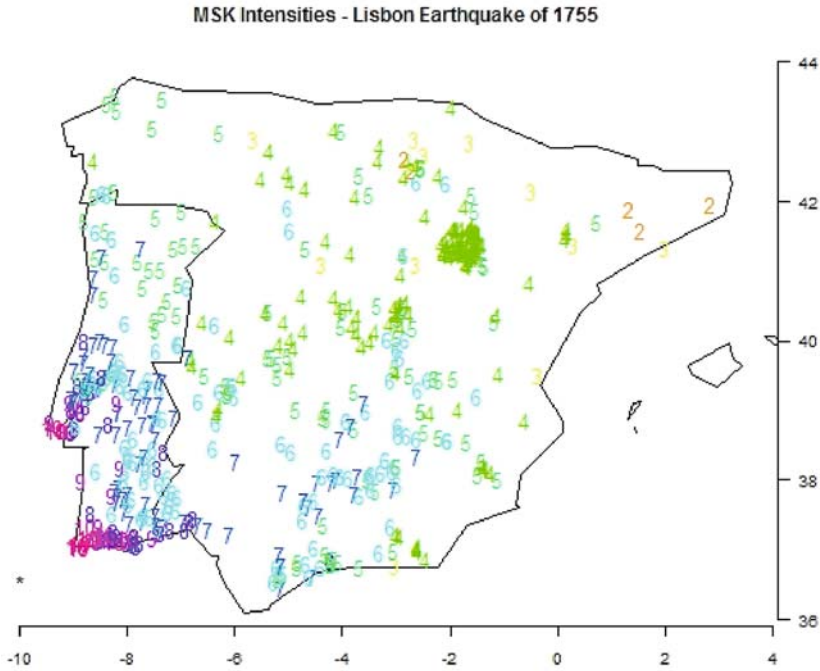


**Fig. 2** Locations and recorded intensity values. The  $x$ - and  $y$ -axes are longitude and latitude respectively. The “\*” is the estimated epicentre of the event

MSK scale is integer-valued only the integer-valued intensities are employed in the computations of the paper. One sees a modal value of  $IV$ . The histogram dips at  $V+$  and  $VI+$ . They may be the result of statistical fluctuations or instead underassignment of the half values. The count at  $X$ , which stands out, is surely due to there being many damageable buildings close to the epicentre.

Figure 2 shows the locations of the measurements for the integer intensities. The clusters of values are associated with population centers. One sees a falloff from level  $X$  to level  $II$  as one moves north and east from the estimated epicentre denoted by “\*” in the figure. It is located in the lower left corner and its coordinates have been taken from (Martinez-Solares and Lopez-Arroyo 2004). There is a lot of intermingling of different levels and overprinting.

### 3 The Statistical Methods Employed

A variety of statistical methods have been employed to develop the results of the paper. They are now described, in part. Statistical techniques have proven useful in addressing problems of insurance, risk management and seismic engineering, in particular those based on random process concepts. These

include those of point processes for damage locations. A representation for a spatial point process is provided by

$$Y(x, y) = \sum_j \delta(x - x_j, y - y_j) \tag{1}$$

with  $\delta$  the Dirac delta function. One for the so-called marked point process is

$$Y(x, y) = \sum_j M_j \delta(x - x_j, y - y_j) \tag{2}$$

In the present case the marks,  $M_j$ , provide a measure of the severity of the event. The mark values are elements in the set  $\{II, III, IV, \dots, X\}$ . Both specific and general models have been developed for point and marked point processes and these processes are basic to probabilistic seismic risk assessment, (Ogata 1983), (Vere-Jones 1992), (Schoenberg and Bolt 2000).

For ordinal data the grouped continuous model, (McCullagh and Nelder 1989), (Agresti 1996) is effective. It involves, a latent (or state) random variable,  $\zeta$  and cutpoints  $\theta_j$ . It leads to representing intensity data values,  $Y$ , as

$$\begin{aligned} Y &= II \text{ if } \zeta \leq \theta_{II} \\ &= j \text{ if } \theta_{j-1} < \zeta \leq \theta_j \text{ if } j = II, III, \dots, IX \\ &= X \text{ if } \theta_{IX} \leq \zeta \end{aligned} \tag{3}$$

for  $j = 1, \dots, J$  with  $\theta_0 = -\infty, \theta_0 = \infty$ . The  $\theta_j$  are to be increasing. There are  $J$  cells.

An important advantage of this model is that an explanatory variable  $X$  may be introduced directly by setting

$$\zeta = -\beta'X + \varepsilon \tag{4}$$

with  $\beta$  a coefficient to be determined from the data.

If one assumes that  $\varepsilon$  has an extreme value distribution, i.e.  $\text{Prob}\{\varepsilon < a\} = 1 - \exp(-e^a)$ , then

$$\text{Prob}\{Y = j | X\} = \exp\{-\exp\{\theta_{j-1} + \beta'X\}\} - \exp\{-\exp\{\theta_j + \beta'X\}\} \tag{5}$$

The use of an extreme value distribution may be motivated by the character of the situation. Its reasonableness may be checked empirically, see Fig. 3 below. For the model (5) the  $\beta$ 's and the  $\theta$ 's may be obtained using functions in standard statistical programs. (In the work of this paper the statistical package R was employed, (Venables and Ripley 2002 and Wood 2006). To do so one represents the likelihood of the data as a product of binomial likelihoods, see page 170 in (McCullagh and Nelder 1989). In the computations reported a modified form of the R function logitreg of (Venables and Ripley 2002), the

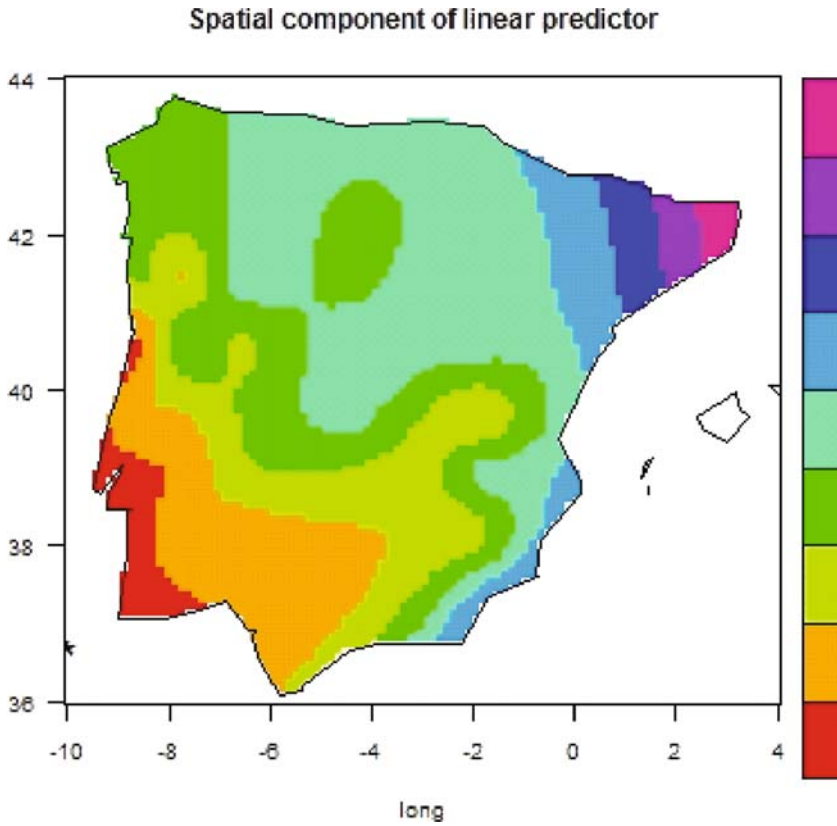


**Fig. 3** The estimated spatial effect  $\beta(x,y)$  of the model (2.5), (2.8). The colors at the top of the legend correspond to larger values

log link and the binomial distribution were used. In this extreme value case an estimate of  $E\{\zeta|X\}$  is provided by

$$-b'X + \gamma \tag{6}$$

where  $b$  is the estimate of  $\beta$  and  $\gamma$  is Euler's constant. In the spatial case at hand one takes

$$\beta'X = \beta(x,y) \tag{7}$$

with  $j$  intensity,  $x$  longitude and  $y$  latitude and  $\beta(x,y)$  smooth. The function  $\beta(x,y)$  may be interpreted as a proxy for variables, such as geology, left out of the model. From expression (5) one has

$$\text{Prob}\{Y(x,y) \leq j|(x,y)\} = 1 - \exp\{-\exp\{\theta_j + \beta(x,y)\}\} \tag{8}$$

One notes that this increases with  $\theta$  and  $\beta$ .  
 In summary the statistical model to be employed is

$$\text{Prob}\{Y(x, y) = j|(x, y)\} = \pi_j(x, y|\theta, \beta) \tag{9}$$

with  $\pi_j(x,y)$  of parametric form and given by expression (5) above. With the assumptions indicated the model forms a so-called generalized linear model (glm) (Wood 2006), and various inference procedures are available. In the results presented  $\beta(x,y)$  will be approximated by a thin-plate spline.

Statistical concepts and techniques of R include ones for the estimation of parameters, for model validation, and for uncertainty computation. The estimation methods include maximum likelihood and parametric and nonparametric fitting. In fact there are several general methods that may be employed to evaluate the uncertainty associated with the estimates. These include: linearization, the jackknife and the bootstrap. Perhaps the easiest to employ here is the jackknife. It involves temporarily deleting data points in groups, computing the estimates for the remaining data points and then combining these values, (Mosteller and Tukey 1977).

## 4 Results

Consideration turns to fitting the grouped continuous model with the distribution (5), (8). The estimate used employs the thin-plate spline approximation to  $\beta(x,y)$ , namely

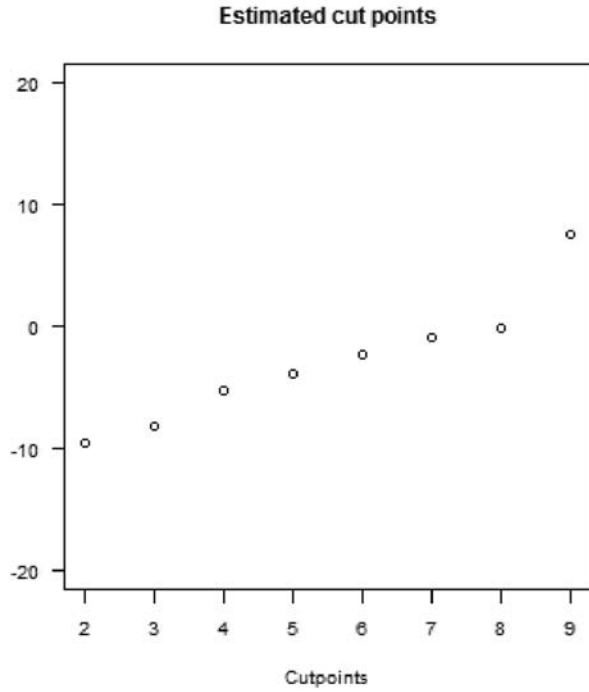
$$\sum_k \beta_k r_k^{-2} \log r_k \tag{10}$$

where for nodes  $(x_k, y_k)$  the variable  $r_k^2 = (x-x_k)^2 + (y-y_k)^2$  and the  $\beta_k$  are parameters to be estimated. The  $(x_k, y_k)$  were taken to lie in a grid covering the peninsula. The expression (10) has the form  $\beta'X$  and maximum likelihood estimation may be employed.

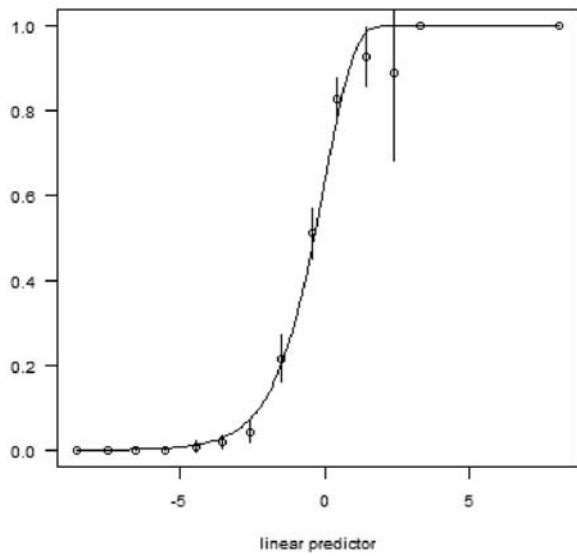
Figure 4 is the estimate of the linear predictor component  $\beta(x,y)$ . Its interpretation is a background representing a smooth regional effect, in the presence of the cutpoint terms. The breakpoints for the color legend have been taken as uniformly spaced across the range of values of the estimate. One sees the estimate to tilt up from the lower left to the upper right. In interpretations of the result one needs to remember that the  $\theta$ 's are also in the model and that possibly there is an interaction between level and location.

Figure 5 provides the estimates of the  $\theta_j$  of model (5), (8). Approximate  $\pm 2$  s.e. limits are indicated by the vertical lines. The estimated  $\theta_j$  are seen to be increasing steadily, approximately linearly. The estimate of  $\theta_{IX}$  is highly variable.

**Fig. 4** The estimated  $\theta_j$ .  
Approximate  $\pm 2$  standard error limits have been added



**Empirical Probability vs. Linear Predictor**



**Fig. 5** Empirical Probabilities and the extreme value distribution function

Sometimes MMI values are treated as if they were numerical, for example being used as the dependent values in least squares analyses such as the model

$$Y = \beta(x, y) + \varepsilon \tag{11}$$

where  $Y$  is the intensity in arabic numerals,  $\varepsilon$  is noise and  $\beta(x,y)$  is smooth, instead of (5), (8).

It is necessary to assess the goodness of fit on any statistical model. Figure 6 provides the results of one study of the model (5). Having picked cells for the fitted linear predictor,  $\theta_j + \beta(x,y)$ , one plots the proportion of cases in a given cell versus the cell's midpoint. The continuous curve is the cumulative distribution function of the extreme value distribution. Also  $\pm 2$  standard error limits have been added to the proportions. The fit seems reasonable for this method of assessment.

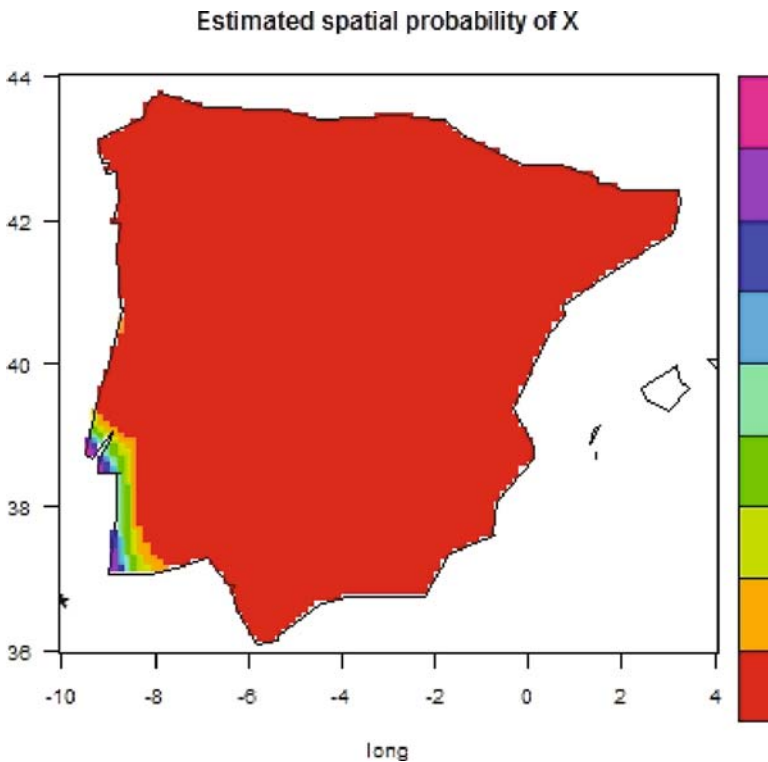


**Fig. 6** Estimated probability for MSK intensity  $X$  as a function of location. The legend on the right goes from 0 at the bottom to 1 at the top

### 5 Uses of the Fitted Model

Once one has a specific stochastic model there are a variety of things that can be done.

For a given location one can now estimate the probabilities of the various MSK intensities occurring employing expression (5). Figures 6, 7, and 8 provide estimates for the particular cases of intensities *X*, *VII* and *II* respectively.

Unsurprisingly the estimate of the probability of intensity *X* is notable only in the southwest corner of the figure, the region closest to the hypercenter.

Next is the figure for intensity *VII*. The notable intensity *VII* probabilities are spread out in the southwest region of the map, but not at the southwest tip. This can be seen for the observed values in Fig. 5.

Lastly, Fig. 8 provides an estimate of  $\text{Prob}\{I = III \mid (x,y)\}$  is plotted. The values are near 1 in the northeast corner but not at the northeast tip. This is consistent with Fig. 4 only showing *IIs* in that corner.

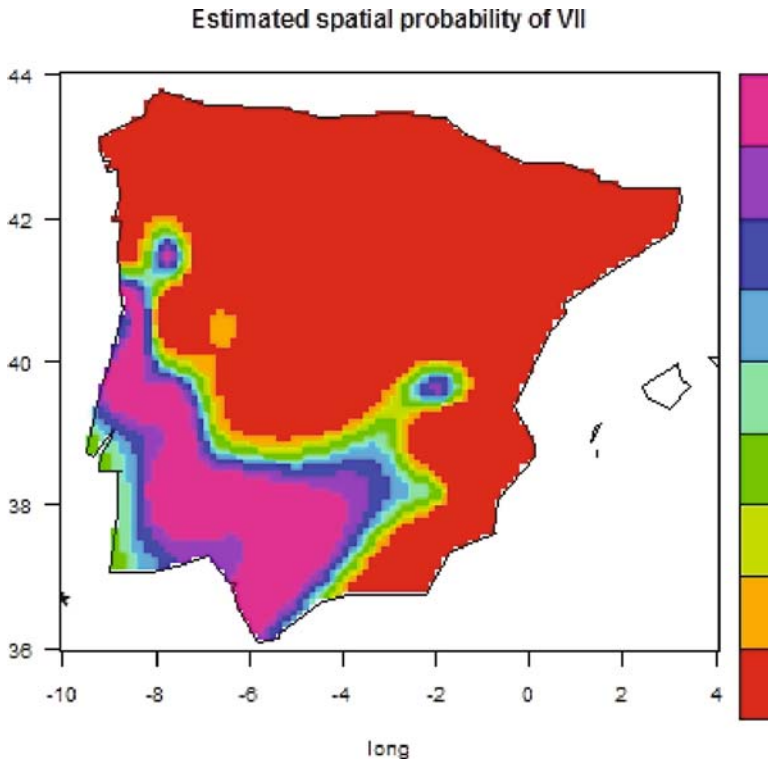


Fig. 7 Estimated probabilities for intensity VII

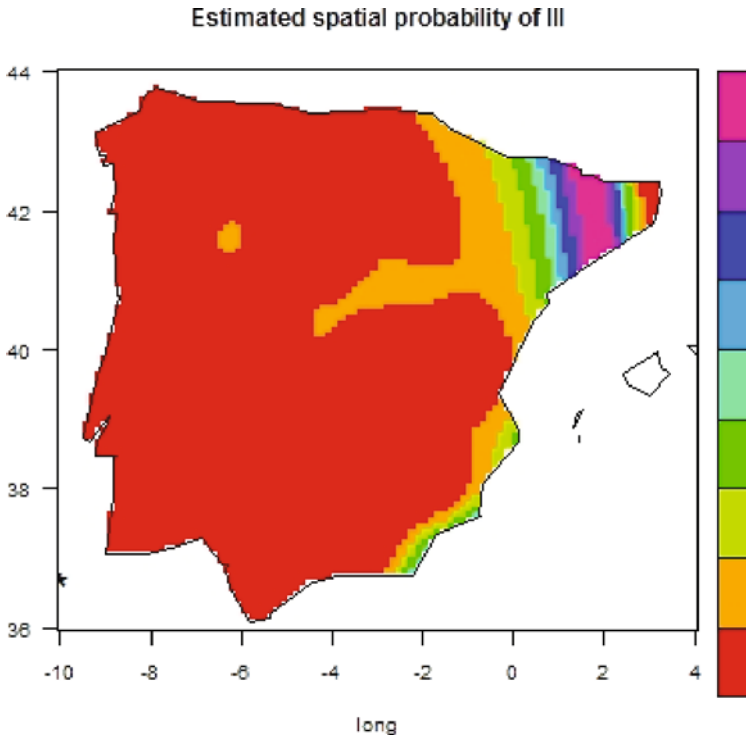


Fig. 8 Estimated probabilities for intensity II

There are other uses for fitted statistical models. Consider how the MSK intensity falls off with the distance of a location from the hypocenter of the event. Figure 9 is a scatter plot of intensity against the logarithm of the distance. One sees a general falloff in the intensity level as the distance increases with a great range in variability for any specific level.

As estimates of falloff in risk with distance from source are important in seismic engineering problems it is worth developing a specific model. An example of the development of estimates for ordinal data is provided in (Brillinger 1997), and (Brillinger 2003).

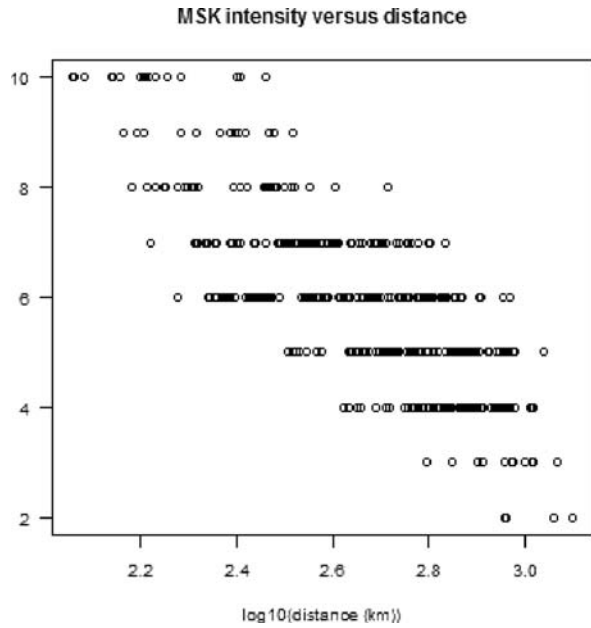
Sometimes it is more convenient to work with distance  $d$  than  $(x,y)$ . (Bolt 2006). For the Lisbon 1755 data the following model will be considered,

$$\text{Prob}\{Y = j|d\} = \exp\{-\exp\{\theta_{j-1} + \gamma(d)\}\} - \exp\{-\exp\{\theta_j \gamma(d)\}\} = \pi_j(d) \quad (12)$$

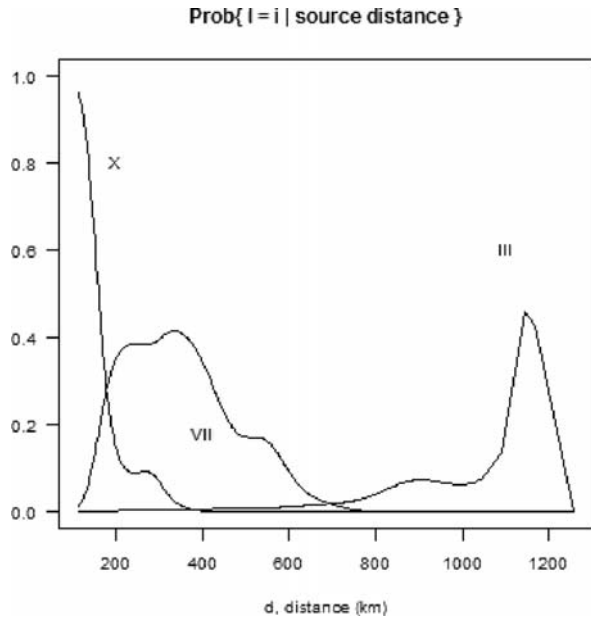
for  $j = II, III, \dots, X$  with  $d$  distance and  $\gamma$ , assumed smooth, expressed as a B-spline, (Venables and Ripley 2002).

Figure 10 provides the results for the 1755 event and the particular cases of intensities  $X, VII$ , and  $III$ . In the case of intensity  $X$  one sees concentration of probability in the region on the land closest to the event. The other

**Fig. 9** Intensity values versus distance from the source



probabilities are largest at intermediate distances across the peninsula. This was apparent in Figure 6. The closest point on the land is approximately 114 km from the hypocenter. The intensity *VII* probabilities peak around



**Fig. 10** Probability of a given intensity occurring as a function of distance from the estimated hypocenter for intensities III, VII and X

350 km and the intensity *III* curve quickly rises and then drops around 1100 km. All told the results are consistent with Fig. 5. At a given distance, the probabilities of intensities *II* through *X* sum to 1.

### 6 Other Derived Values

Having a statistical model one may compute statistical properties and displays for other quantities of interest. As an example consider the maximum acceleration. Empirical relations have been derived relating it to intensity.

As an example (Bolt 2006, Appendix C) provides some characteristic peak velocity and acceleration values as follows

The figures of Table 2 may be put together with the fitted probability model to obtain an estimated distribution for the maximum acceleration as a function of distance. Specifically, suppose intensities *II* and *III* are neglected. Then let  $a_j$  denote a characteristic value for the  $j$ -th row in the table,  $j = J$ , with  $X$  standing for  $X$ -*XII*. Let  $Y = (Y_1, \dots, Y_J)$  denote a multinomial variate with  $j$ -th probability,  $\pi_j(d)$ , at (9) above. The acceleration at distance  $d$  may be approximated by

$$A(d) = \sum_j a_j Y_j \tag{13}$$

and distributional properties determined from those of the multinomial. For example the expected acceleration at distance  $d$  is approximated by

$$\sum_j a_j \pi_j(d) \tag{14}$$

Another quantity is percent risk/damage or damageability matrix, (Munich Re 1991) providing loss ratios (Table 3) for three classes of buildings as a percent. (vulnerability)

**Table 2** Peak velocities and accelerations associated with given MMIs

MMI	<i>IV</i>	<i>V</i>	<i>VI</i>	<i>VII</i>	<i>VIII</i>	<i>IX</i>	<i>X-XII</i>
vel (cm/sec)	1-2	2-5	5-8	8-12	20-30	45-66	>60
accel (g)	.015-.02	.03-.04	.06-.07	.10-.15	.25-.30	.50-.55	>.60

**Table 3** Percentage losses. Taken taken from (Munich Re, 1991)

MMI	<i>VI</i>	<i>VII</i>	<i>VIII</i>	<i>IX</i>	<i>X</i>
residential	.4	1.7	6	17	42
commercial	.8	3	11	27	60
industrial	.1	.7	3	11	30

An expression like (12) above may be employed to evaluate probabilities associated with loss percentages.

## 7 Discussion and Conclusions

For many years isoseismals have been produced by hand. This paper presents an objective statistical approach to evaluating related quantities, specifically probabilities that a particular intensity value occurs at a particular location. As well as being less subjective it is computerized thus allowing rapid production of figures. The approach makes specific use of the information that the intensity scale is ordinal. These may be fed into estimations of quantities such as of loss ratios, occurring in later stages of risk analyses

The study has limitations. Bias may be mentioned. This would occur if for a case of damage the probability that it would go unrecorded depended on the location  $(x,y)$ . (However if that probability could be estimated then the bias could be corrected for.) Next one can remark that the methods employed were based on assumed models. These may not hold. In particular the extreme value distribution had particular computational convenience, but others may prove useful. The smoothing methods involved tuning parameters, which need to be chosen. However the greatest limitation is not including other explanatory variables in the model. It was hoped to have site conditions, and geology and Professor Bolt was working on this when he died.

**Acknowledgments** Bruce Bolt was a very strong proponent of the use of statistical methods in seismology and seismic engineering. He introduced me to many of the important concepts of those fields. It is hard to find words of gratitude for his having shared his knowledge with me. This paper would have been so much better had he not died so suddenly.

Bob Wiegel, another Berkeley colleague, helped me to understand some of the research concerned with locating the source of the earthquake. J. M. Martinez-Solares, and J. M. Miranda provided the intensity data employed in the study. I thank them also.

The research was supported by the NSF grants DMS-20010831 and DMS-20051127.

## References and Further Readings

- Agresti A (1996) *An Introduction to Categorical Data Analysis*. Wiley, New York.
- Baptista MA, Miranda JM, Chierici F, Zitellini (2003) New study of the 1755 earthquake source based on multi-channel seismic survey data and tsunami modelling. *Natural Hazards and Earth System Science* 3: 333–340.
- Bolt BA (2006) *Earthquakes, Fifth Edition*. Freeman, New York.
- Brillinger DR (1993) Earthquake risk and insurance. *Environmetrics* 4: 1–21.
- Brillinger DR (1997) Random process methods and environmental data: the 1996 Hunter Lecture. *Environmetrics* 8: 269–281.
- Brillinger DR (2003) Three environmental probabilistic risk problems. *Statistical Science* 18: 412–421.

- Brillinger DR, Chiann C, Irizarry RA, Morettin PA (2001) Automatic methods for generating seismic intensity maps. *Journal Applied Probability* 38A: 188–201.
- Bullen KE, Bolt BA (1985) *An Introduction to the Theory of Seismology*, Fourth Edition. Cambridge U. Press, Cambridge.
- De Rubeis V, Gasparini C, Maramai I, Murru M, Tertulani A (1992) The uncertainty and ambiguity of isoseismal maps. *Earthquake Engineering Structural Dynamics* 21: 509–523.
- Hastie TJ, Tibshirani RJ (1990) *Generalized Additive Models*. Chapman and Hall, London.
- Joyner WB, Boore DM (1981) Peak horizontal acceleration and velocity from strong motion records from 1979 Imperial Valley, California. *Bulletin Seismological Society of America* 71: 2011–2038.
- Martinez-Solares JM, Lopez-Arroyo A (2004) The great historical 1755 earthquake, effects and damages in Spain, *Journal of Seismology* 8: 275–294.
- McCullagh P, Nelder JA (1989) *Generalized Linear Models*, Second Edition. Chapman and Hall, New York.
- Mendes-Victor LA, Baptista MA, Miranda JM, Miranda PM (1999) Can Hydrodynamic Modelling of Tsunami Contribute to Seismic Risk Assessment? *Phys. Chem. Earth* 24: 139–144.
- Mosteller F, Tukey JW (1977) *Data Analysis and Regression*. Addison-Wesley, Reading.
- Munich Re. Insurance and Reinsurance of the Earthquake Risk. Munich Re, Munich. 1991.
- Ogata Y (1983) Likelihood analysis of point processes and its application to seismological problems. *Bulletin International Statistical Institute* 50: 943–961.
- Perkins JB, Boatwright J (1995) *On Shaky Ground*. ABAG, Oakland.
- Pettenati F, Sirovich L, Cavallini F (1999) Objective treatment and synthesis of macroseismic intensity data sets using tessellation. *Bulletin Seismological Society of America* 98: 1203–1213.
- Reiter L (1990) *Earthquake Hazard Analysis*. Columbia, New York.
- Schoenberg F, Bolt B (2000) Short-term exciting, long-term correcting models for earthquake catalogs. *Bulletin Seismological Society of America*, 99: 849–858.
- Sokolov VY, Chernov KY (1998) On the correlation of seismic intensity with Fourier amplitude spectra. *Earthquake Spectra* 14: 679–694.
- Venables WN, Ripley BD (2002) *Modern Applied Statistics with S*, Fourth Edition. Springer, New York.
- Vere-Jones D (1992) Statistical methods for the description and display of earthquake catalogues. *Statistics and Environmental Sciences* (eds. A. T. Walden and P. Guttorp) Halstead, New York, pp. 220–246.
- Wald D, Quitariano V, Dengler LA, Dewey JW (1999) Utilization of the internet for rapid community intensity maps. *Seismology Research Letters* 70: 680–697.
- Wood SN (2006) *Generalized Additive Models: An Introduction with R*. Chapman and Hall, New York.